Journal of
Polymer Materials

Tech Science Press

DOI: 10.32604/jpm.2024.055397

ARTICLE

Extraction and Detailed Physico-Chemical Characterization of Lignocellulosic Fibers Derived from *Lonchocarpus cyanescens*

Edja Florentin Assanvo[1,*], Kanga Marius N'GATTA[1], Kicoun Jean-Yves N'zi Touré[1,2,3], Amenan Sylvie Konan[4] and David Boa[4]

[1]Laboratoire de Thermodynamique et Physico-Chimie des Matériaux, Université Nangui ABROGOUA, Abidjan 02, 02 PB 801, Côte d'Ivoire

[2]Department of Physics, Kenyatta University, Nairobi, P.O. Box 43844-00100, Kenya

[3]Department Civil, Environmental and Architectural Engineering, Worcester Polytechnic Institute, Worcester, MA 01609-2280, USA

[4]Laboratoire de Valorisation de la Diversité Végétale, Université Nangui ABROGOUA, Abidjan 02, 02 PB 801, Côte d'Ivoire

*Corresponding Author: Edja Florentin Assanvo. Email: aedjaflorentin@gmail.com

Received: 26 June 2024 Accepted: 24 July 2024 Published: 09 August 2024

ABSTRACT

The present study focused on extraction of *Lonchocarpus cyanescens* (*L. cyanescens*) fiber (LCF) and the physico-chemical properties of the obtained fiber. The fiber was extracted by manual and traditional rating methods, treated with sodium hydroxide, and characterized to determine its performance properties. The chemical composition of cellulose, hemicellulose, and lignin was determined according to the acid detergent, neutral detergent, and Klason methods, respectively. The results show significant quantities of cellulose (33%), hemicellulose (30%), and lignin (24%) in the studied fibers. LCF exhibited a porous multicellular and poly lamellate network structure (FE-SEM) with a crystallinity index of 56.5%. The thermal stability using TGA analysis indicates that the maximum and main degradation temperature is 325°C. The crystallinity, thermal stability, and opening of micropores on the fiber surface have been increased after alkaline treatment. As a conclusion drawn, LCF fibers could be used as potential reinforcement in polymer matrices for a variety of applications where porous, multicellular, and poly lamellate network structure is needed.

KEYWORDS

Lonchocarpus cyanescens fiber; extraction; physicochemical properties; polylamellate network

1 Introduction

Population growth and industrial expansion have led to the intensive and abusive use of fossil fuels. This raises major concerns about its long-term supply, the erratic price of petroleum products, and, in particular, its environmental footprint. To alleviate these concerns, worldwide efforts are being made to raise awareness among populations and industrialists regarding the use of resources within the general framework of sustainable development. Leading to a strong interest in the use of clean

technologies for the development of high-potential products in production chains by the researchers and industrials communities. In addition, there are undoubtedly numerous environmental and human restrictions associated with the use of fossil fuel resources, but the advantages generated by the usage of agro-resources outweigh them. Agro-resources are biodegradable, inexpensive, environmentally friendly, and also harmless to health [1,2]. Among the possible agro-based alternatives, plant fibers offer numerous advantages and fit in perfectly with global trends in resource and energy management. Plant fiber and derivatives can be used as reinforcements in polymer matrices for a wide range of applications, including energy storage [3,4], biomedical [5–9], packaging [10,11], construction industry [12,13], automotive, aeronautics, sports and leisure, etc. [6,8,14–17]. Indeed, the interest in plant fibers is also related to their abundance, renewability, biodegradability, and non-polluting characteristics, as their low cost, low density, and high rigidity [14,15]. They can be extracted from various plant parts such as leaves, roots, bark, fruit, bast, stems, etc. [12,18]. As a result, there is a wide diversity of plant species that can be used to produce fibers suitable for use in industrial applications [12,18]. However, their morphology and mechanical properties vary according to botanical species, geographical location, origin, age, extraction procedure, and processing methods used [18–20]. The commonly studied and compiled plant fibers in the literature include cotton, flax, hemp, jute, kenaf, sisal, ramie, coir, banana, pineapple leaf, bagasse, wheat straw, etc. [12,21], widely used in composite materials elaboration [12,16,22]. However, the current scale of production of these fibers cannot fully cover the demand of the industries, hence the need to explore new sources of plant fibers with adequate properties to meet the current need. For this purpose, the scientific community still searching all over the world for natural fibers that are locally available in various geographical areas. These fibers could also be a source of additional local population's income. The utilization of untreated plant fibers is often hindered by several factors. These raw fibers exhibit high hygroscopicity, low durability and thermal stability, and insufficient mechanical strength [23]. To address these limitations, various physical, chemical, and biological treatments have been developed to modify the properties of natural fiber matrices and surfaces [24–26]. However, the impact of these treatments on the surface, mechanical, and biofunctional properties of different natural fibers remains unclear. This complexity arises from the unique chemical composition of each fiber type, which is primarily influenced by its genotype, cultivation conditions, and harvesting practices [18–20,24].

Among the diverse treatment methods available, alkaline treatment with sodium hydroxide (NaOH) stands out as one of the most widely employed approaches [25,27]. This method effectively removes non-cellulosic constituents, such as hemicellulose and lignin, along with impurities like waxes and oils [27]. The presence of these undesirable elements adversely affects the properties of plant fiber-based composites. Their degradation in alkaline environments compromises fiber durability, leading to a decline in the composite's long-term strength and structural stability [25]. Consequently, their elimination during the pre-treatment stage proves beneficial for the overall performance of the composite. Alkaline treatment with NaOH offers additional advantages beyond the removal of non-cellulosic components. It also induces defibrillation, resulting in a rougher fiber surface [28]. This increased roughness enhances mechanical interlocking between the fiber and the matrix, optimizing the wettability of the fiber by the matrix. These synergistic improvements contribute to an overall enhancement of the fiber's performance within composites [25,26].

In the present study, we report on a new plant fiber extracted from *Lonchocarpus cyanescens (L. cyanescens*). *L. cyanescens* is a climbing shrub of the Fabaceae family native to the forests and savannahs of Africa, a deciduous plant containing indoxyl, which yields the indigotin contained in the dye indigo [29]. Apart from this usual use, *L. cyanescens* is used in African ethnomedicine for the treatment of several infections such as skin diseases, leprosy, ulcers, yaws, diabetes, diarrhea, treatment of bone pain, boils, anti-arthritic conditions [29].

Up to today, *L. cyanescens* plant has merely been studied for their phytochemical properties [29]. However, their fibers remain unknown heretofore to the scientific world in order to draw the best profile from them. Therefore, with the aim of solving the growing demand for plant fibers, the present study was undertaken to document information on the physico-chemical characteristics of fiber extracted from the *L. cyanescens* plant. This study will provide the database needed to plan a compilation of its industrial applications. To this end, embarking on an uncharted territory, this study delves into the unexplored realm of fibers derived from the *L. cyanescens* plant. With meticulous precision, we unravel the intricate tapestry of their physicochemical, thermal, and surface properties. Furthermore, we embark on a journey to decipher the potential functional properties of these fibers by subjecting them to alkaline treatment, meticulously examining their transformative impact on their matrix and surface characteristics.

2 Experimental

2.1 Materials

L. cyanescens stem sample was collected at Toumodi in the central of Côte d'Ivoire, and identified by botanists at the Centre Nationale de Floristique (CNF) of the University of Félix Houphouët, Abidjan, Côte d'Ivoire. The chemical used were sodium hydroxide (98%) and sulphuric acid (H_2SO_4, 72%) from SD Fine Chem Limited, MA, USA.

2.2 Fiber Extraction

The tree was cut in piece and immersed in water for 7 days with 2% of NaOH. After, the stem was separate with the tree and by manual and traditional rating, fiber was extracted and combed before drying in sunlight for 3 days.

2.3 Alkaline Fiber Treatment

Chemical modification of *L. cyanescens* fibers (LCF) was performed using the mercerization technique as reported in the literature [30,31] and then adapted to our study. Briefly, 10 g LCF was immersed in 300 mL NaOH solution (5%) for 1 h at room temperature and then filtered. The residue obtained was then washed with distilled water and rinsed with methanol to remove the remaining sodium hydroxide. Finally, the resulting fibers were again rinsed with distilled water in order to reach a neutral pH (pH = 7), filtered under vacuum and dried at 105°C in an oven for 24 h to give the treated fibers noted LCF-T.

2.4 Fiber Characterization

2.4.1 Chemical Composition

The chemical composition of untreated (LCF) and treated *L. cyanescens* fiber was examined according to the standard test methods reported by Guna et al. [32] and then adapted to our study. In fact, cellulose and hemicellulose contents were determined according to the acid detergent and neutral detergent methods. Briefly, 100 mL of a neutral detergent solution was softly added to 1 g of finely ground fiber sample. The resulting solution was then heated under continuous stirring for 1 h, filtered by vacuum suction and then washed with hot water to remove all traces of the detergent. The residue obtained was oven-dried for 24 h at 105°C to give neutral detergent fibers (NDF). The mass of NDF represents that of the cellulose contained in the samples. A similar procedure was followed to determine hemicellulose content, replacing the neutral detergent solution with acid detergent. Lignin content was determined by the Klason method (TAPPI T211 om-83). To this end, 300 mg (W) of fiber was suspended in 3 ml sulfuric acid (H_2SO_4, 72%) for 1 h at room temperature (30°C). Next, 84 mL

of 18 M MilliQ water was added to the suspension, then heated to reflux at 121°C for 4 h. After acid hydrolysis, the residue was washed to neutralize the pH, filtered, dried in an oven (105°C, 24 h) and weighed to calculate the percentage of lignin. To determine ash content, 3 g of fibers were burnt in a ceramic crucible using a muffle furnace at 550°C for 5 h. The ash percentage was calculated on the basis of the residual ash weight.

2.4.2 X-Ray Diffraction (XRD)

An X-ray diffraction (XRD) study was carried out on the LCF and LCF-T samples using X-ray diffractometer (model Miniflex II, Rigaku, MA, USA). This analysis was used to determine the crystal structure and crystalline parameters such as crystallinity index, crystallinity percentage and crystallite size. In the present study, the analysis was carried out with Cu-Kα radiation at a wavelength $\lambda = 0.15418$ nm at 40 kV and 30 mA. Scanning speed was 0.5° min^{-1}. Diffraction spectra were recorded over a range of angles 2θ varying from 5° to 50° then processed with Origin Pro software and peak intensities identified.

The crystallinity index (*CrI*) (Eq. (1)) and percentage crystallinity (Eq. (2)) were determined using Segal's empirical method [33,34], known as the peak height method.

$$CrI = \frac{I_{200} - I_{am}}{I_{200}} \times 100 \tag{1}$$

$$\%Cr = \frac{I_{200}}{I_{200} + I_{am}} \times 100 \tag{2}$$

where I_{200} and I_{am} represent the maximum intensities in the crystalline and amorphous regions, respectively, i.e., the lowest between the (110) and (200) planes at $2\theta \approx 20°$). The inter-reticular distance (Eq. (3)), i.e., the lattice spacing (d_{hkl}) and crystallite size (L) (Eq. (4)), were determined by Bragg's law and Scherer's law, respectively [35–39].

$$d\,(nm) = \frac{n\lambda}{2\sin\theta} \tag{3}$$

where n is the order of refraction ($n = 1$); λ wavelength of the radiation beams (0.15418 nm) and θ the Bragg angel.

$$L\,(nm) = \frac{K\lambda}{\beta\cos\theta} \tag{4}$$

K is the Scherer constant (0.9), λ wavelength of the radiation beams (0.15418 nm), β is the width at half maximum (FWHM) in radians of the crystal peak deconvoluted at the crystallographic plane (200) and θ the scattering Bragg angel in radians.

2.4.3 Fourier Transform Infrared (FTIR) Spectroscopy

The functional groups present in the LCF and LCF-T samples were analyzed by Fourier transform infrared spectrometry (FTIR) (Jasco, Model No-4700, CSIR, Chennai, India) in attenuated total reflectance (ATR) mode. All spectra were recorded in the 4000–500 cm^{-1} spectral range, with an accumulation of 32 scans at 4 cm^{-1} resolution at room temperature.

2.4.4 Morphological Observation

Morphological observation was carried out on LCF and LCF-T to assess alkali-induced changes in *L. cyanescens* fibers. The morphologies of the samples were examined with field emission scanning electron microscope (FESEM) measurements (model-CLARA, TESCAN, Kohoutovice, Czech

Republic) equipped with an energy-dispersive X-ray spectroscope (EDX). Prior to SEM observation, the samples were sputtered with a thin layer of gold to avoid the charging effects of the electron beam during examination.

2.4.5 Thermal Analysis

The thermal behavior of the samples was analyzed using a TGA/DSC system (model STA 449 F3 Jupiter®, NETZSCH, CSIR, Chennai, India) under a nitrogen atmosphere flowing at 100 mL/min. This analysis was used to assess the thermal stability of untreated and treated fibers in terms of sample mass loss. The temperature range used was 30°C to 600°C, with a heating rate of 10°C/min. For each test, a sample of approximately 8 mg of previously dried ground fibers was used.

3 Results and Discussions

3.1 Chemical Composition

The chemical composition of *L. cyanescens* fibbers is reported in Table 1 and presented as follow, (33 ± 3) % cellulose, (30 ± 3) % hemicellulose, (24 ± 2) % lignin and 4% ash. The relatively high lignin content (24 ± 2%) suggests that *L. cyanescens* fiber resists to microbial attack, giving it high structural rigidity [15]. A comparative analysis of the chemical composition of *L. cyanescens* fiber with other natural fibers is reported in Table 1 showing that *L. cyanescens* fibers contains a relatively lower cellulose content than many other known natural fibers. However, *L. cyanescens* fibers contains a higher cellulose content than *Stipa obtuse* [31] and close to that of sugarcane bagasse fiber, Coffee hull, Teff straw [20], *Calamus tenuis* [15], etc. The mechanical properties of fibers extracted from natural resources depend essentially on their cellulose content [40].

Table 1: Chemical composition of *L. cyanescens* fiber and comparison with other plants

Fibers	Chemical composition				Ref.
	Cellulose	Hemicellulose	Lignin	Ash	
LCF	33 ± 3	30 ± 3	24 ± 2	4	This study
Cyperus campactus	67.9	19.5	12.6		[40]
Calamus tenuis	37.4 ± 1.4	31.06 ± 1.03	28.42 ± 0.81	4.11 ± 0.62	[15]
Stipa obtusa	29.54	27.57	23.76	3.52	[31]
Mikania micrantha	56.42	21.42	15.78		[41]
Chanvre	66.71	20.02	4.92		[42]
Lin	69.18	19.85	8.40		
Thespesia populnea barks	70.12	12.64	16.34	1.80	[35]
Cissus quadrangularis stem	82.73	7.96	11.27		[19]
Cissus quadrangularis root	77.17	11.02	10.45		
Pennisetum Alopecuroides	40	29.5	19.66	6.76	[43]
Ramie (Boehmeria nivea)	68–76	14–18	4–7		[44]
Kigelia africana	55.1 ± 0.2	9.34 ± 0.08	11.7 ± 0.2		[36]
Furcraea foetida	68.35	11.46	11.46		[28]
Coccinia grandis L.	62.35	13.42	15.61		[45]
Agave Americana	68.54 ± 3.46	18.41 ± 2.28	6.08 ± 3.39		[46]
Bamboo bleached pulp	79.34 ± 2.1	15.10 ± 1.3	0.08 ± 0.003		[47]
sabai grass	42.9 ± 0.6	21.1 ± 1.0	18.5 ± 1.6		[32]
Acacia mangium	47.1 ± 0.1	31.1 ± 0.5	23.0 ± 0.2		[33]

(Continued)

Table 1 (continued)

Fibers	Chemical composition				Ref.
	Cellulose	Hemicellulose	Lignin	Ash	
Teff straw	36.7 ± 0.55	23.6 ± 0.88	19.5 ± 1.02		[20]
Enset fiber	60.0 ± 1.25	18.5 ± 0.68	10.7 ± 0.65		
Sugarcane bagasse	39.5 ± 1.08	23.4 ± 1.24	21.0 ± 0.95		
Coffee hull	35.5 ± 1.80	14.8 ± 1.10	30.7 ± 0.36		

3.2 X-Ray Diffraction (XRD)

The XRD profiles of the LCF and LCF-T samples are shown in Fig. 1 and the crystal parameters are recorded in Table 2. All samples show diffraction peaks at 2θ ≈ 16°, 18°, 24° and 31°, corresponding respectively to the (1$\bar{1}$0), (110), (200) and (004) crystal planes of the cellulose Iβ monoclinic structure [31,41,48–50]. This implies that the LCF crystal structure was unaltered after the alkaline treatment. Furthermore, a valley has been detected in the diffractograms at 2θ ≈ 20°, suggesting that LCF and LCF-T exhibit amorphous regions [30,35,39]. Thus, these peaks prove the semi-crystalline nature of LCF and LCF-T. This semi-crystalline nature of the fibers could be the result of the substantial presence of amorphous components such as hemicellulose, lignin and amorphous cellulose in the fiber structure. The crystallinity index and percentage of LCF evaluated using Segal's method are 56.5% and 69.7%, respectively. These relatively low values justify the high proportion of amorphous components (hemicellulose, lignin and amorphous cellulose). However, the alkali modified the crystalline parameters such as the index and percentage crystallinity of LCF. The index and percentage crystallinity of LCF-T are estimated at 76.2% and 80.7%, respectively. These values are higher than those of LCF. These parameters increased refers to the removal of fiber amorphous regions, which occurs as a result of the partial degradation of lignin, hemicellulose and amorphous cellulose [31]. However, the crystallinity index of LCF is poroche of that of Spathes of male date (57.82%) [39] and *Cissus quadrangularis* (59.22%) [19] but higher than many plant fibers such as *Calamus tenuis* (37.38 ± 0.27) [15], *Coccinia grandis* stem (46.09%) [51], *Stipa obtusa* (45.63%) [31], Moroccan *Pennisetum Alopecuroides* plan (49.14%) [43], etc., and smaller than that of *Corypha taliera* fruit (62.5%) [52], *Calotropis gigantea* Bast Fibers (80.09%) [53], Hemp (88%) [54].

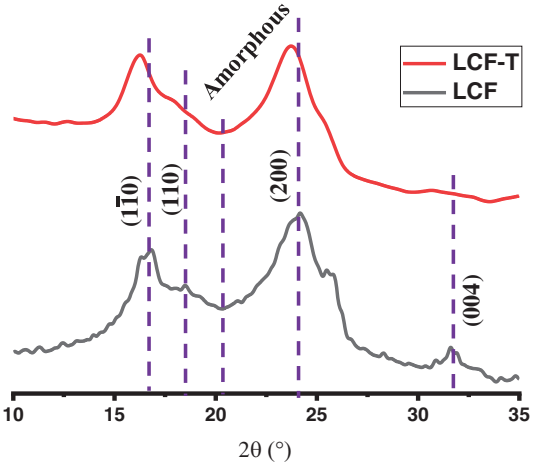

Figure 1: XRD diffractograms of LCF and LCF-T

Table 2: Crystallographic parameters of L. *cyanescens* fiber

Samples	*CrI*	% *CrI*	L (nm)	$d_{(200)}$ (nm)
LCF	56.55	69.71	1.81	0.367
LCF-T	76.16	80.75	0.47	0.374

The crystallite sizes of LCF and LCF-T calculated from the Scherrer equation are at 1.81 and 0.47 nm, respectively. LCF crystallite size is comparable to that of *F* rattan (*Calamus manan*) (1.91 nm) [55], but smaller than that of *Thespesia populnea* fibers (3.576 nm) [35], *Cyperus compactus* Retz (7.61 nm) [40].

3.3 Fourier Transform Infrared Spectroscopy (FT-IR)

According to the chemical composition analysis, *L. cyanescens* fibers are composed mainly of cellulose, hemicellulose and lignin. These structural components of plant fibers consist of esters, aromatic cetones and alcohols, with different oxygen-containing functional groups [31,52]. In order to confirm the chemical composition of and assess the effect of alkali treatment, FT-IR analysis was performed onto LCF and LCF-T samples. Fig. 2 shows the infrared spectra of LCF and LCF-T. All infrared characteristics are shown in Table 3. Analysis of the spectra reveals a broad absorption band, to know in the range of 3500 and 3250 cm^{-1} attributed to OH stretching of the alcohol functional group of the cellulose and water present in the fibers [19,43]. The absorption band observed at around 2890 cm^{-1} corresponds to the vibration of the C-H stretching of cellulose and hemicellulose [56]. The absorption peak at 2135 cm^{-1} is attributed to the presence of water and CO_2 bending [19], while the one observed at around 1730 cm^{-1} is attributed to the C=O carbonyl stretching of the ester or carbonyl groups of the hemicellulose components present in LCF [40,43]. The intense particle peak at around 1630 cm^{-1} could be dedicated to water uptake by the fiber [56,57]. The vibrational peaks observed at 1435 and 1335 cm^{-1} respectively indicate vibrations of asymmetric-CH3 stretching and C-O stretching of acetyl groups of the aromatic plane of lignin components in LCF lignin or C-O stretching of hemicellulose [15,40]. The broad band between 1150 and 1000 cm^{-1} attests to the presence of the C-OH vibration [41] while the absorption peak observed at around 890 cm^{-1} indicates the presence of the C-O-C stretching of the β (1-4)-glycosidic bonds of the pyranose ring backbone of cellulose [52,56]. In view of the above, it is worth noting that FT-IR spectra confirm the presence of cellulose, hemicellulose and lignin in LCF. However, in the LCF-T spectrum, the peak intensities of the absorption bands characteristic of cellulose increased, while those corresponding to the functional groups characteristic of hemicellulose and lignin decreased. This means that NaOH treatment tends to remove non-cellulosic components such as hemicellulose and lignin to obviously give a more cellulose-rich fiber residue. A similar trend has been reported by various heights regarding the effect of NaOH on various plant fibers [30,36,58].

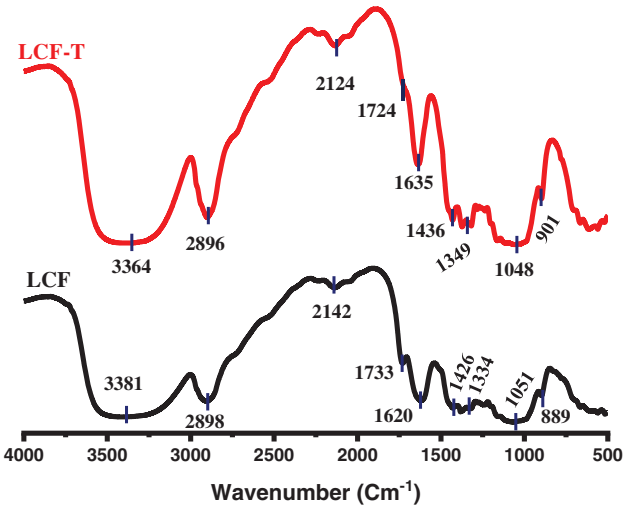

Figure 2: FTIR plotted results of LCF and LCF-T

Table 3: Infrared characteristics of *L. cyanescens* fiber

FTIR peak origin	Wavenumbers (cm^{-1})	
	LCF	LCF-T
O-H stretching of the alcohol functional group of the cellulose	3381	3364
C-H stretching of cellulose and hemicellulose	2898	2896
CO_2 stretch	2142	2134
C=O stretch of acetyl group of hemicellulose	1733	1724
OH of cellulose and water	1620	1635
Vibrations of asymmetric-CH_3 stretching of lignin	1434	1436
C-O stretching of acetyl groups of lignin or hemicellulose	1334	1349
C-OH vibration	1051	1048
C-O-C stretching of the β (1-4)-glycosidic bonds of cellulose	889	901

3.4 Morphological Observation

Fig. 3 shows the surface micrographs of LCF and LCF-T. These FE-SEM images show that *L. cyanescens* fibers present a regularly arranged multicellular and polylamellate network with corners of varying shapes from oval to round. This type of morphology has been observed in other natural fibers such as *Cyperus compactus* [40], *Pennisetum alopecuroides* [43], *Chloris barbata* [59], *Citrullus lanatus* [60] Sugar palm *(Arenga pinnata (Wurmb.) Merr)* [58], *Coccinia grandis* stem [51]. The morphological view of presented by the FE-SEM image in Fig. 3a reveals that *L. cyanescens* crude fibers (LCF) present a non-uniform porous surface and contain impurities due to the presence of undesirable amorphous components such as hemicellulose and lignin. Conversely, the micrograph in Fig. 3b shows that alkali eliminates surface impurities and improves micropore dispersion on the LCF-T surface, which indicates that NaOH treatment induces the elimination of surface impurities and consequently improves the surface morphology of the plant fibers. Same observations has already been made by various authors on other plant fibers [25,43]. The removal of surface impurities and the

homogeneous dispersion of micropores due to alkali treatment are the interest of the present. Indeed, the elimination of surface impurities and the dispersion of micropores onto the fiber surface could offer an advantage for LCF-T to serve as reinforcement for polymer matrices in composite applications [61]. In addition, lignin and hemicellulose form the outer layer of the plant fiber due to their function as binding substances. Their removal therefore leads to an increase in the contact surface of the cellulose fiber with the matrix, and could consequently ensure greater adhesion of the fiber to the matrix or increase the internal bonding strength.

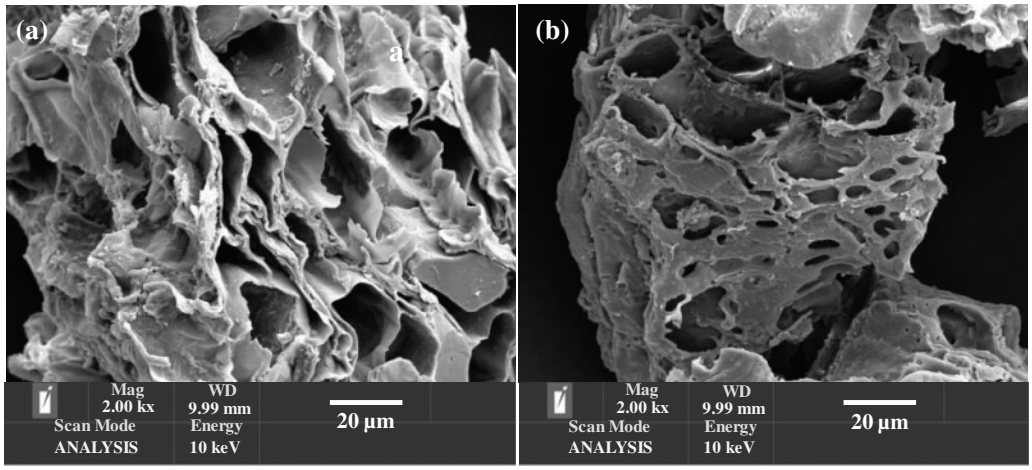

Figure 3: SEM images of LCF (a) and LCF-T (b)

3.5 Thermogravimetry Analysis (TGA)

To evaluate the prospective use of LCF, we studied the thermal stability of LCF and LCF-T in order to predict the most suitable conversion process. Indeed, the three main basic lignocellulosic fiber components, namely cellulose, hemicellulose and lignin, control its thermal stability, and their order of stability is state as follows: hemicellulose < cellulose < lignin [31,56]. Hemicellulose decomposition predominates at 250°C–330°C, while cellulose and lignin decomposition occurs between 330°C and 570°C, and at temperatures above 570°C, lignin decomposition predominates [31]. However, it is worth pointing out that lignin degradation is more complex, as it can start at around 160°C and extend up to 900°C due to the activities of its various chemical bonds [31,40]. In the present study, the thermal stability of the sample fibers was investigated by TG/DTG analysis, and the thermograms are shown in Fig. 4. As a result, the LCF and LCF-T samples show three stages of thermal degradation in line with the literature [36,52]. In LCF, the first degradation step occurred at around 60°C accompanied by a mass loss of 6%, while that of LCF-T is observed at around 97°C for 11% mass loss. This degradation step is attributed to moisture evaporation due to the intrinsic hydrophilic character of lignocellulosic fibers, and to the volatilization of low molecular weight compounds [19,31]. Subsequently, the fibers remained thermally stable up to around 225°C and 255°C for LCT and LCF-T, respectively. This suggests that alkali improves the thermal stability of the lignocellulosic fiber probably due to the removal of hemicellulose [30] as well as some surface impurities materials. In the second stage, losses of 59% and 49% were recorded on the ATG curves of LCF and LCF-T, respectively, with major decomposition observed at 325°C and 344°C, respectively. This relatively large mass loss observed is attributed to the simultaneous degradation of hemicellulose and cellulose [39,40]. The maximum degradation peak observed on the DTG curves was mainly due to cellulose degradation [39].

Finally, the third stage of degradation relates to lignin decomposition [40,31] with around 9% and 10% mass loss respectively for LCF and LCF-T.

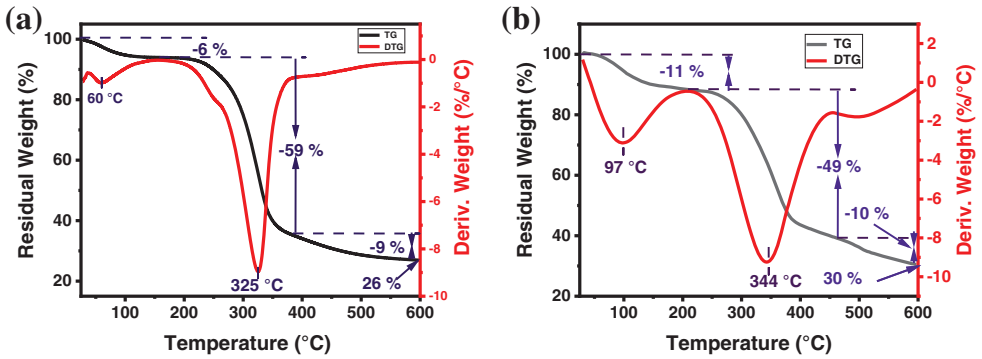

Figure 4: TGA (black) and DTG (red) curves of LCF (a) and LCF-T (b)

In view of its thermal characteristics, it is worth pointing out that *L. cyanescens* fiber could be used as a reinforcement in matrices for which processing or use temperatures are below 225°C.

4 Conclusion

In the present study, a new lignocellulosic fiber was extracted from the plant of *L. cyanescens*, treated with NaOH solution (5% N) and then characterized. Various conclusions can be drawn from the above-mentioned analytical results. *L. cyanescens* fiber is porous and contains a relatively low cellulose content of around 33%, embedded in a matrix of hemicellulose (30%) and lignin (24%). FTIR analysis confirmed that *L. cyanescens* fiber is composed of cellulose, hemicellulose and lignin, while XRD analysis revealed its semi-crystalline nature. Thermal analysis revealed that LCF is stable up to around 225°C. After alkali treatment, some of the unwanted amorphous compounds such as hemicellulose and lignin were removed, as shown by FTIR, XRD and TGA/DSC analysis to give fibers with properties such as improved crystallinity and thermal stability. Compared with the crude fiber (LCF), NaOH treatment enabled the opening of micropores on the surface and stability of the *L. cyanescens* fiber up to around 255°C. This could give *L. cyanescens* fiber an additional advantage as a reinforcement for polymer matrices with melting temperatures below 255°C.

Due to its remarkable properties, *L. cyanescens* fiber shows great promise as a reinforcing material for a wide range of polymer composites. Its multilayer and porous structure, coupled with its enhanced thermal stability after alkaline treatment, makes it particularly suitable for applications where these characteristics are crucial. Here are some specific examples of potential applications:

Packaging: *L. cyanescens* fiber could be used to reinforce packaging, making it stronger, lighter, and more durable. This would reduce the use of traditional packaging materials, such as plastic, and thus contribute to environmental protection.

Particleboard and plywood: *L. cyanescens* fiber could be used to reinforce particleboard and plywood, making them stronger, stiffer, and lighter. This would reduce the use of solid wood and thus contribute to forest conservation.

Biomedical field: *L. cyanescens* fiber could be used to make biodegradable scaffolds for tissue regeneration, orthopedic implants, and other biomedical devices. Its biocompatibility and porous structure make it an ideal material for these applications.

In addition to these examples, *L. cyanescens* fiber could find applications in many other fields, such as the automotive industry, aerospace, and construction. Future research will focus on optimizing the properties of *L. cyanescens* fiber and developing new composites based on this fiber for specific applications.

In conclusion, *L. cyanescens* fiber is a renewable and promising material with a wide range of potential applications. Its development could contribute to the creation of more sustainable and environmentally friendly products.

Acknowledgement: The authors feel thankful to Central Leather Research Institute, Chennai, India where the laboratory experiments have been done, and the President of University Nangui Abrogoua, Abidjan, Cote d'Ivoire.

Funding Statement: This research received no specific grant from any public, commercial, or non-profit funding agencies.

Author Contributions: Edja Florentin Assanvo: Methodology, Validation, Investigation, Resources, Data Curation, Writing-Review & Editing, Visualization. David Boa: Methodology, Supervision, Writing—Review & Editing. Amenan Sylvie Konan: Investigation, Validation. Kicoun Jean-Yves N'zi Touré: Investigation, Validation, Writing—Review & Editing. Kanga Marius N'GATTA: Investigation, Methodology, Writing-Original Draf. All authors reviewed the results and approved the final version of the manuscript.

Availability of Data and Materials: The datasets generated during and/or analyzed during the current study are available from the corresponding author on reasonable request.

Ethics Approval: Not applicable.

Conflicts of Interest: The authors declare that they have no conflicts of interest to report regarding the present study.

References

1. Jaiswal D, Devnani GL, Rajeshkumar G, Sanjay MR, Siengchin S. Review on extraction, characterization, surface treatment and thermal degradation analysis of new cellulosic fibers as sustainable reinforcement in polymer composites. Curr Res Green Sustain Chem. 2022;5:100271. doi:10.1016/j.crgsc.2022.100271.
2. Florentin E, Yves KJ, Toure NZ, Marius K, Gatta N. Kinetic and thermodynamic study of composite with jute fiber as reinforcement. Int J Renew Energy Dev. 2024;13(1):1–9.
3. Sharma A, Thakur M, Bhattacharya M, Mandal T, Goswami S. Commercial application of cellulose nanocomposites–a review. Biotechnol Rep. 2019;21:e00316. doi:10.1016/j.btre.2019.e00316.
4. Muddasar M, Beaucamp A, Culebras M, Collins N. Cellulose: characteristics and applications for rechargeable batteries. Int J Biol Macromol. 2022;219(5):788–803. doi:10.1016/j.ijbiomac.2022.08.026.
5. Patil TV, Patel DK, Dutta SD, Ganguly K, Santra TS, Lim KT. Nanocellulose, a versatile platform: from the delivery of active molecules to tissue engineering applications. Bioact Mater. 2022;9:566–89. doi:10.1016/j.bioactmat.2021.07.006.
6. Ferreira FV, Otoni CG, De France KJ, Barud HS, Lona LMF, Cranston ED, et al. Porous nanocellulose gels and foams: breakthrough status in the development of scaffolds for tissue engineering. Mater Today. 2020;37:126–41. doi:10.1016/j.mattod.2020.03.003.
7. Courtenay JC, Filgueiras JG, Deazevedo ER, Jin Y, Edler KJ, Sharma RI, et al. Mechanically robust cationic cellulose nanofibril 3D scaffolds with tuneable biomimetic porosity for cell culture. J Mater Chem B. 2019;7(1):53–64.
8. Surendran G, Sherje AP. Cellulose nanofibers and composites: an insight into basics and biomedical applications. J Drug Deliv Sci Technol. 2022;75:103601. doi:10.1016/j.jddst.2022.103601.
9. N'Gatta KM, Belaid H, El Hayek J, Assanvo EF, Kajdan M, Masquelez N, et al. 3D printing of cellulose nanocrystals based composites to build robust biomimetic scaffolds for bone tissue engineering. Sci Rep. 2022;12(1):1–14. doi:10.1038/s41598-022-25652-x.

10. Noremylia MB, Hassan MZ, Ismail Z. Recent advancement in isolation, processing, characterization and applications of emerging nanocellulose: a review. Int J Biol Macromol. 2022;206(1):954–76. doi:10.1016/j.ijbiomac.2022.03.064.
11. Silva FAGS, Dourado F, Gama M. Nanocellulose bio-based composites for food packaging. Nanomaterials. 2020;10:2041.
12. Abdalla JA, Hawileh RA, Bahurudeen A, Jyothsna G, Sofi A, Shanmugam V, et al. A comprehensive review on the use of natural fibers in cement/geopolymer concrete: a step towards sustainability. Case Stud Constr Mater. 2023;19(1):e02244. doi:10.1016/j.cscm.2023.e02244.
13. Kumar R, Kumar R, Purohit R, Sinha R. Natural fibre reinforced composite materials: environmentally better life cycle assessment–a case study. Mater Today Proc. 2020;26(2):3157–60. doi:10.1016/j.matpr.2020.02.651.
14. Viscusi G, Barra G, Verdolotti L, Galzerano B, Viscardi M, Gorrasi G. Natural fiber reinforced inorganic foam composites from short hemp bast fibers obtained by mechanical decortation of unretted stems from the wastes of hemp cultivations. Mater Today Proc. 2021;34(1):176–9. doi:10.1016/j.matpr.2020.02.672.
15. Kar A, Saikia D. Characterization of new natural cellulosic fiber from *Calamus tenuis* (Jati Bet) cane as a potential reinforcement for polymer composites. Heliyon. 2023;9(6):e16491. doi:10.1016/j.heliyon.2023.e16491.
16. Dua S, Khatri H, Naveen J, Jawaid M, Jayakrishna K, Norrrahim MNF, et al. Potential of natural fiber based polymeric composites for cleaner automotive component production—a comprehensive review. J Mater Res Technol. 2023;25(6):1086–104. doi:10.1016/j.jmrt.2023.06.019.
17. Oluwarotimi S, Akpan E, Dhakal HN. Review on natural plant fibres and their hybrid composites for structural applications: recent trends and future perspectives. Compos Part C Open Access. 2022;9(10):100322. doi:10.1016/j.jcomc.2022.100322.
18. Jeyapragash R, Srinivasan V, Sathiyamurthy S. Mechanical properties of natural fiber/particulate reinforced epoxy composites—a review of the literature. Mater Today: Proc. 2020;22(3):1223–7. doi:10.1016/j.matpr.2019.12.146.
19. Manimekalai G, Kavitha S, Divya D, Indran S, Binoj JS. Characterization of enzyme treated cellulosic stem fiber from *Cissus quadrangularis* plant: an exploratory investigation. Curr Res Green Sustain Chem. 2021;4(1–3):100162. doi:10.1016/j.crgsc.2021.100162.
20. Gabriel T, Belete A, Syrowatka F, Neubert RHH, Gebre-Mariam T. International journal of biological macromolecules extraction and characterization of celluloses from various plant byproducts. Int J Biol Macromol. 2020;158:1248–58. doi:10.1016/j.ijbiomac.2020.04.264.
21. Hamidon MH, Sultan MTH, Ariffin AH, Shah AUM. Effects of fibre treatment on mechanical properties of kenaf fibre reinforced composites: a review. J Mater Res Technol. 2019;8(3):3327–37. doi:10.1016/j.jmrt.2019.04.012.
22. Akter T, Hossain MS. Application of plant fibers in environmental friendly composites for developed properties: a review. Clean Mater. 2021;2(8):100032. doi:10.1016/j.clema.2021.100032.
23. Zamora-Mendoza L, Gushque F, Yanez S, Jara N, Álvarez-Barreto JF, Zamora-Ledezma C, et al. Plant fibers as composite reinforcements for biomedical applications. Bioengineering. 2023;10(7):1–23.
24. Alsafran M, Sadasivuni KK, Haneesh JM, Razavi MM, Kasote DM. Extraction and characterization of biofunctional lignocellulosic fibers from *Pulicaria undulata* plant and the effect of alkali treatment on their bio-physicochemical properties. Carbohydr Polym Technol Appl. 2024 Jul;8(3):100542. doi:10.1016/j.carpta.2024.100542.
25. Dhasindrakrishna K, Pasupathy K, Ramakrishnan S, Sanjayan J. The ambient and elevated temperature performance of hemp fibre reinforced alkali-activated cement foam: effects of fibre dosage and alkali treatment. J Build Eng. 2023;76(11):107131. doi:10.1016/j.jobe.2023.107131.
26. Latif R, Wakeel S, Khan NZ, Noor Siddiquee A, Lal Verma S, Akhtar Khan Z. Surface treatments of plant fibers and their effects on mechanical properties of fiber-reinforced composites: a review. J Reinf Plast Compos. 2019;38(1):15–30.
27. Karim FE, Islam MR, Supto MH, Rafi AAM, Tanni TR, Begum HA. Surface modification of Luffa and Maize fibers by using alkali medium. Clean Eng Technol. 2024;19:100736. doi:10.1016/j.clet.2024.100736.

28. Manimaran P, Senthamaraikannan P, Sanjay MR, Marichelvam MK. Study on characterization of *Furcraea foetida* new natural fiber as composite reinforcement for lightweight applications. Carbohydr Polym. 2018;181(3):650–8. doi:10.1016/j.carbpol.2017.11.099.
29. Adeoye AT, Adedapo AA, Abatan MO. Study on acute ulcerous pain in rats treated with aqueous root extract of *Lonchocarpus cyanescens*. J Acute Dis. 2016;5(6):454–7. doi:10.1016/j.joad.2016.09.002.
30. Guo A, Sun Z, Satyavolu J. Impact of chemical treatment on the physiochemical and mechanical properties of kenaf fibers. Ind Crop Prod. 2019;141:111726. doi:10.1016/j.indcrop.2019.111726.
31. Chavez BK, Garces-Porras K, Parada DC, Flores E. Thermochemical isolation and characterization of nanofibrillated cellulose from *Stipa obtusa* fibers. Carbohydr Polym Technol Appl. 2023;6(2):100344. doi:10.1016/j.carpta.2023.100344.
32. Guna V, Ilangovan M, Adithya K, Akshay Koushik CV, Srinivas CV. Bio fibers and biocomposites from sabai grass: a unique renewable resource. Carbohydr Polym. 2019;218:243–9.
33. Jasmani L, Adnan S. Preparation and characterization of nanocrystalline cellulose from *Acacia mangium* and its reinforcement potential. Carbohydr Polym. 2017;161(3):166–71. doi:10.1016/j.carbpol.2016.12.061.
34. Segal L, Creely JJ, Martin AE Jr, Conran CM. An empirical method for estimating the degree of crystallinity of native cellulose using the X-ray diffractometer. Text Res J. 1958;29(10):786–94.
35. Kathirselvam M, Kumaravel A, Arthanarieswaran VP, Saravanakumar SS. Isolation and characterization of cellulose fibers from *Thespesia populnea* barks: a study on physicochemical and structural properties. Int J Biol Macromol. 2019;129(1):396–406. doi:10.1016/j.ijbiomac.2019.02.044.
36. Ilangovan M, Guna V, Prajwal B, Jiang Q, Reddy N. Extraction and characterisation of natural cellulose fibers from Kigelia Africana. Carbohydr Polym. 2020;236:115996. doi:10.1016/j.carbpol.2020.115996.
37. Adel A, El-shafei A, Ibrahim A, Al-shemy M. Extraction of oxidized nanocellulose from date palm (*Phoenix dactylifera* L.) sheath fibers: influence of CI and CII polymorphs on the properties of chitosan/bionanocomposite films. Ind Crop Prod. 2018;124(4):155–65. doi:10.1016/j.indcrop.2018.07.073.
38. Khanjanzadeh H, Park B-D. Optimum oxidation for direct and efficient extraction of carboxylated cellulose nanocrystals from recycled MDF fibers by ammonium persulfate. Carbohydr Polym. 2021 Jan;251(5):117029. doi:10.1016/j.carbpol.2020.117029.
39. Lamia B, Nafissa M, Abdelouahab Djoubair B, Jawaid M, Fouad H, Midani M. New cellulosic fibre from Spathes of male date for lightweight composite materials: extraction and characterization. J Mater Res Technol. 2023;24:5361–71. doi:10.1016/j.jmrt.2023.04.159.
40. Bhunia AK, Mondal D, Sahu KR, Mondal AK. Characterization of new natural cellulosic fibers from *Cyperus compactus* Retz. (Cyperaceae) plant. Carbohydr Polym Technol Appl. 2023;5:100286. doi:10.1016/j.carpta.2023.100286.
41. Shrestha UR, Mamontov E, Neill HMO, Zhang Q, Alexander I. Extraction and characterization of a newly developed cellulose enriched sustainable natural fiber from the epidermis of *Mikania micrantha*. Innovation. 2022;23(1):100199. doi:10.1016/j.xinn.2021.100199.
42. Świątkiewicz M, Zimniewska M, Różańska W, Gryszczyńska A, Kołodziej J, Młocek W, et al. Assessment of flax and hemp fibres in terms of their impact on the growth performance and health status of weaned piglets. Animal. 2022;16(12).
43. Elmoudnia H, Faria P, Jalal R, Waqif M, Saadi L. Effectiveness of alkaline and hydrothermal treatments on cellulosic fibers extracted from the Moroccan *Pennisetum Alopecuroides* plant: chemical and morphological characterization. Carbohydr Polym Technol Appl. 2023;5(17):100276. doi:10.1016/j.carpta.2022.100276.
44. Suriaman I, Hendrarsakti J, Mardiyati Y, Darmawan A. Synthesis and characterization of air filter media made from cellulosic ramie fiber (*Boehmeria nivea*). Carbohydr Polym Technol Appl. 2022;3(3):100216. doi:10.1016/j.carpta.2022.100216.
45. Senthamaraikannan P, Kathiresan M. Characterization of raw and alkali treated new natural cellulosic fiber from *Coccinia grandis. L*. Carbohydr Polym. 2018;186(20):332–43. doi:10.1016/j.carbpol.2018.01.072.
46. Madhu P, Sanjay MR, Jawaid M, Siengchin S, Khan A, Pruncu I. A new study on effect of various chemical treatments on Agave Americana fiber for composite reinforcement: physico-chemical, thermal, mechanical and morphological properties. Polym Test. 2020;85(1):106437. doi:10.1016/j.polymertesting.2020.106437.
47. Seta FT, An X, Liu L, Zhang H, Yang J, Zhang W, et al. Preparation and characterization of high yield cellulose nanocrystals (CNC) derived from ball mill pretreatment and maleic acid hydrolysis. Carbohydr Polym. 2020;234(70):115942. doi:10.1016/j.carbpol.2020.115942.

48. Xing L, Hu C, Zhang W, Guan L, Gu J. Transition of cellulose supramolecular structure during concentrated acid treatment and its implication for cellulose nanocrystal yield. Carbohydr Polym. 2020;229(1):115539. doi:10.1016/j.carbpol.2019.115539.
49. Gökben Başaran Kankılıç AÜM. Phragmites australis as a new cellulose source: extraction, characterization and adsorption of methylene blue. J Mol. 2020;312:113313.
50. Lan J, Chen J, Zhu R, Lin C, Ma X, Cao S. Antibacterial and antiviral chitosan oligosaccharide modified cellulosic fibers with durability against washing and long-acting activity. Int J Biol Macromol. 2023;231(3):123587. doi:10.1016/j.ijbiomac.2023.123587.
51. Jebadurai SG, Raj RE, Sreenivasan VS, Binoj JS. Comprehensive characterization of natural cellulosic fiber from Coccinia grandis stem. Carbohydr Polym. 2019;207:675–83, Elsevier Ltd. doi:10.1016/j.carbpol.2018.12.027.
52. Tamanna TA, Belal SA, Shibly MAH, Khan AN. Characterization of a new natural fiber extracted from Corypha taliera fruit. Sci Rep. 2021;11(1):1–13. doi:10.1038/s41598-021-87128-8.
53. Ramasamy R, Obi Reddy K, Varada Rajulu A. Extraction and characterization of *Calotropis gigantea* bast fibers as novel reinforcement for composites materials. J Nat Fibers. 2018;15(4):527–38. doi:10.1080/15440478.2017.1349019.
54. Moshi AAM, Ravindran D, Bharathi SRS, Indran S, Saravanakumar SS, Liu Y. Characterization of a new cellulosic natural fiber extracted from the root of *Ficus religiosa* tree. Int J Biol Macromol. 2020;142(1):212–21. doi:10.1016/j.ijbiomac.2019.09.094.
55. Ding L, Han X, Cao L, Chen Y, Ling Z, Han J, et al. Characterization of natural fiber from manau rattan (*Calamus manan*) as a potential reinforcement for polymer-based composites. J Bioresour Bioprod. 2022;7(3):190–200. doi:10.1016/j.jobab.2021.11.002.
56. Hossain S, Jalil MA, Islam T, Rahman MM. A low-density cellulose rich new natural fiber extracted from the bark of jack tree branches and its characterizations. Heliyon. 2022;8(11):e11667.
57. Ajayi SM, Olusanya SO, Sodeinde KO, Didunyemi AE, Atunde MO, Fapojuwo DP, et al. Hydrophobic modification of cellulose from oil palm empty fruit bunch: characterization and application in Pickering emulsions stabilization. Carbohydr Polym Technol Appl. 2023;5(9):100282. doi:10.1016/j.carpta.2023.100282.
58. Ahmad R, Mohd S, Ibrahim R, Abral H, Roslim M, Huzaifah M, et al. Sugar palm (*Arenga pinnata* (Wurmb.) Merr) cellulosic fibre hierarchy: a comprehensive approach from macro to nano scale. Integr Med Res. 2019;8(3):2753–66. doi:10.1016/j.jmrt.2019.04.011.
59. Balasundar P, Narayanasamy P, Senthamaraikannan P, Senthil S, Prithivirajan R, Ramkumar T. Extraction and characterization of new natural cellulosic *Chloris barbata* fiber. J Nat Fibers. 2018;15(3):436–44. doi:10.1080/15440478.2017.1349015.
60. Khan A, Vijay R, Singaravelu DL, Sanjay MR, Siengchin S, Jawaid M, et al. Extraction and characterization of natural fibers from *Citrullus lanatus* climber. J Nat Fibers. 2022;19(2):621–9. doi:10.1080/15440478.2020.1758281.
61. Ahmed J, Balaji MA, Saravanakumar SS, Senthamaraikannan P. A comprehensive physical, chemical and morphological characterization of novel cellulosic fiber extracted from the stem of *Elettaria Cardamomum* plant. J Nat Fibers. 2021;18(10):1460–71. doi:10.1080/15440478.2019.1691121.